

Supplementary Information

Differential signaling networks of Bcr-Abl p210 and p190 kinases in leukemia cells defined by functional proteomics

Running title: **Differential signaling of Bcr-Abl p210 and p190**

Sina Reckel¹, Romain Hamelin², Sandrine Georgeon¹, Florence Armand²,
Qinfang Jolliet², Diego Chiappe², Marc Moniatte² and Oliver Hantschel^{1,3}

¹ Swiss Institute for Experimental Cancer Research (ISREC), School of Life Sciences, École polytechnique fédérale de Lausanne (EPFL), 1015 Lausanne, Switzerland

² Proteomics Core Facility, School of Life Sciences, École polytechnique fédérale de Lausanne (EPFL), 1015 Lausanne, Switzerland

³ ISREC Foundation Chair in Translational Oncology

Content

Supplementary Materials and Methods

Supplementary Tables S1-S7 (extended versions as Excel file)

Supplementary Table S8 (provided as Excel file only)

Supplementary Figures S1-S8

Supplementary Materials and Methods

Cell lines and antibodies

The murine pro B-cell line BaF3 (DSMZ ACC-300) was retrovirally transduced with the human Bcr-Abl p210 and p190 cDNAs. In contrast to the parental cells, the transduced cells become interleukin 3 (IL3)-independent and are cultured in the absence of this growth factor. Un-transduced parental BaF3 cells were cultured in the presence of 100 ng/mL mL3. Human cell lines used in this study are specified in Supplementary Table S3. All cell lines were grown in RPMI1640 medium supplemented with 10-20% fetal bovine serum and 1x Pen/Strep.

Antibodies were purchased at Cell Signaling Technology (Stat3 #9139, pAbl(Y245) #2868, pAbl(Y412) #2865, pLyn(Y507) #2731, pSrc(Y416) #6943, pStat5(Y694) #9359 and pStat3(Y705) #9145), Santa Cruz Biotechnology (adapatin1/2 #sc-177771, Lyn #sc-7274, SHIP-2 #sc-515211, STAT5 #sc-835), Abcam (Lyn #ab1890) and Rockland Immunochemicals (Sts-1 #600-401-870) or prepared in-house and purified on a ProteinG affinity resin (Abl clone 24-21, 4G10).

SILAC (stable isotope labeling with amino acids in cell culture) cell growth

Growth of the three cell lines used in the SILAC experiments - BaF3 parental, BaF3 p210, BaF3 p190 - was optimized for isotope labeling with respect to optimal amino acid concentrations and adaptation time. The optimal growth medium was based on RPMI medium for SILAC (Thermo Scientific, catalogue no. 89984), supplemented with 10% dialyzed FBS (Thermo Scientific, catalogue no. 88440) and 1x Pen/Strep. Amino acids were added at 100 mg/L for Arg, 40 mg/L for Lys and 200 mg/L Pro either unlabeled or labeled according to Supplementary Table S1. On average 9-10 doublings were used to prepare SILAC samples and incorporation rates for Arg and Lys of >95% were achieved. Arg to Pro conversion was minimized by the addition of light proline (200 mg/L) and constituted less than <5% of the signal.

Cells were washed in PBS prior inoculation of the labeled SILAC medium at 1×10^5 cells per mL starting from a 10 mL culture dish. Expansion of the cells up to 550 mL final volume per cell line was achieved in an orbital shaker at 180 rpm. Cell growth was monitored by cell counting in order to make sure the necessary doubling times were achieved. Between $7 \cdot 10^8$ total cells were usually obtained after 7 days. After harvesting the cells by centrifugation (500 xg, 10 min), cells were washed twice in PBS and cell pellets were immediately snap-frozen in liquid nitrogen and stored at -80°C for short term.

Interactome sample preparation by large-scale anti-Abl immunoprecipitation

The optimized final protocol used 80-100 mg total cell lysate per cell line, corresponding to approx. $7 \cdot 10^8$ BaF3 cells. Cell lines and lysates were kept separate and only mixed after elution from the anti-Abl resin in order to avoid exchange of Bcr-Abl/Abl interactors between the samples. In parallel, 50 μg of total cell lysate of each cell line were mixed and used for total protein analysis.

Cell lysis and purification was performed in TAP buffer (50 mM TRIS pH 7.5, 100 mM NaCl, 5% glycerol, 0.2% (w/v) NP-40 Alternative) containing protease and phosphatase inhibitors (25 mM sodium fluoride, 1 mM vanadate, 1 mM PMSF, 10 $\mu\text{g}/\text{mL}$ TPCK, 1x Complete protease inhibitor (Roche)¹. After resuspending the cell pellet in 10 mL TAP buffer per $1 \cdot 10^9$ cells, the lysate was incubated on ice for 10 min prior centrifugation at 20 000 xg, 20 min in a tabletop centrifuge. Protein concentration of the lysates was determined using a Bradford assay and equal mg amounts of each lysates were subsequently used for the immunoprecipitation.

The sepharose resins used for the interactome sample preparation, IgG resin for pre-clearing and anti-Abl for the immunoprecipitation, were freshly prepared and stored at 4°C . For the pre-clearing, normal mouse IgG antibody (Thermo Scientific, catalog no. 10400C) was covalently coupled to NHS-activated sepharose (GE Healthcare, catalogue no. 17-0906-01) at a ratio of 6 mg antibody to 1 mL resin. The same coupling ratio was also used for the monoclonal Abl antibody (clone 24-21)² recognizing a very C-terminal epitope

of Abl in Bcr-Abl and c-Abl. Both resins release only very small amounts of heavy and light chain of the antibody upon acidic elution from the resin, which greatly facilitates mass spectrometry analysis. The lysates were pre-cleared for 1 h at 4°C with the IgG-NHS resin and the supernatant then transferred to the Abl-NHS resin for another 3 h at 4°C. For each immunoprecipitation, 250 μ l IgG resin 500 μ l Abl resin were employed. The resin was washed with a total of 10 column volumes (CV) TAP buffer at 4°C and sequentially eluted with 5x 1 CV of 125 mM HCl. Elution fractions were immediately neutralized with 1 M TEAB buffer in a 1:6 v/v ratio. The five elution fractions were analyzed for the presence of Bcr-Abl complexes by anti-Abl immunoblotting and typically fraction 2 and 3 contained >80% of the total eluted Bcr-Abl complexes (Supplementary Figure S3). Fractions E2 and E3 were thus pooled prior to mixing of the three individual immunoprecipitates of BaF3 parental, p210 and p190 with equal volumes and subsequently lyophilized.

Lyophilized samples were resuspended in 2% SDS (w/v), 50 mM Dithioerythritol (DTE) and digested with endoproteinase LysC (Wako) and Trypsin (Promega) using the Filter Aided Sample Preparation protocol (FASP)³. Digested proteins were further desalted using the C18 Stage Tip procedure and dried by vacuum centrifugation. Peptides were finally fractionated prior to LC-MS2 by the Stage Tip strong cation exchange (SCX) protocol using volatile buffers as described⁴.

Phosphoproteome sample preparation

Cells were grown as described above and aliquots of 1×10^8 cells were frozen at -80°C for short-term storage. Cell lysis was accomplished in Urea buffer (8 M Urea, 50 mM Hepes, pH 7.6, 25 mM sodium fluoride, 1 mM vanadate, 1x Complete protease inhibitor (Roche), 1x HALT phosphatase inhibitor (Thermo)) using 2 mL buffer for 1×10^8 cells. After incubation for 10 min on ice, samples were centrifuged (20 000 xg, 20 min) in a tabletop centrifuge. Protein concentration of the lysates was determined using a Bradford assay.

We then mixed 10 mg of total cell lysate of each sample (light, medium and heavy labeled) to have a final amount of 30 mg SILAC sample for peptide

preparation. The mixed lysates were reduced, alkylated and digested using Lys-C and trypsin according to standard protocols. After desalting, samples were split for the respective downstream application and evaporated by vacuum centrifugation. Of the resulting peptides, two-thirds were used in the pY peptide enrichment. The total proteome analysis was done from a fraction of the remaining sample.

Phosphotyrosine peptides were enriched using a mixture of two phosphotyrosine antibodies: The pY1000 antibody that is part of the PTMScan[®] Phospho-Tyrosine Rabbit mAb (P-Tyr-1000) Kit (Cell Signaling Technologies, catalogue number 8803), in addition to 50 μ L NHS-coupled 4G10 antibody as preliminary tests had indicated a slightly increased number of captured peptides. Coupling of the 4G10 antibody to the NHS-sepharose was done in analogy to the Abl antibody used for the interactome study at a ratio of 6 mg antibody to 1 mL resin. The dried peptides corresponding to 20 mg total cell lysate were resolubilized in 1.2 mL IAP buffer (50 mM MOPS/NaOH pH 7.2, 10 mM Na₂HPO₄, 50 mM NaCl, according to Cell Signaling Technologies). After removing the insoluble parts (10 000 xg, 5 min, 4°C) the supernatant was incubated with the pY antibody resin at 4°C over night. The resin was washed twice with 1x IAP buffer and three-times in H₂O before elution in 0.15% TFA.

Afterwards eluates were desalted using C18 Stage Tips and dried by vacuum centrifugation. A second step of phosphopeptide enrichment was performed on TiO₂ tips as described⁵ and peptides were again desalted by C18 Stage Tip and dried prior MS analysis.

Reverse-Phase Chromatography Mass Spectrometry and Data Processing

For LC-MS/MS analysis, samples were resuspended in 2% acetonitrile (ACN, Biosolve), 0.1% Formic Acid (FA). Each pY enriched sample was injected in duplicates in order to maximize site quantifications between biological replicates. Peptides were trapped for 10 min on a Dionex Acclaim PepMap 100 (Thermo) 75 μ m x 2 cm, C18, 3 μ m, 100 Å pre-column and then separated on a 50 cm reversed phase column (Dionex Acclaim PepMap

RSLC (Thermo) 75 μm x 50 cm, C18, 2 μm , 100 Å) over a 120 or 240 min gradient. Nano flow separations were performed on a Dionex Ultimate 3000 RSLC nanoUPLC system in-line connected with an Orbitrap Q Exactive Mass-Spectrometer (Thermo Fischer Scientific). Data acquisition was performed in a data-dependent mode where the 10 most intense ions with charge states ≥ 2 were sequentially fragmented by High Collision Dissociation HCD using 27% Normalized collision Energy (NCE). Orbitrap MS survey scans resolution was set at 70'000 (at 200 m/z) and fragments were measured at 17'500 resolution. SILAC data were analyzed with MaxQuant⁶ version 1.5.1.2 against a database constituted of the Uniprot mouse database release 2015_04 (53217 entries) and the p210 Bcr-Abl sequence. Enzyme specificity was set to Trypsin and a minimum of seven amino acids was required for peptide identification. Up to two missed cleavages were allowed. A cut-off was fixed at 1% FDR at the peptide and protein identification level.

For the interactome database search carbamidomethylation was set as a fixed modification, whereas oxidation (M), acetylation (protein N-term), Pyro-Glu (N-term Q), Pyro-Glu (N-term E) were considered as variable modifications. Only phosphorylation (STY), oxidation (M) and acetylation (protein N-term) in the phosphoproteome data analysis were considered as variable modifications. SILAC quantifications was performed by MaxQuant using the standard settings and with the re-quantification mode enabled. Significance B (SignB) values were calculated using Perseus Software⁷. Further graphical displays were performed using R statistical computing environment (<https://www.R-project.org/>).

Sample preparation for proteomics data validation and immunoblot analysis

Validation of the interactome proteomics data was done by immunoblot using the BaF3 SILAC cell lines (parental, p210 and p190), an independent set of BaF3 cells as well as the human cell lines specified in Supplementary Table S4. Samples were prepared in analogy to the interactome sample preparation. We probed the total cell lysates of all cell lines for the total expression levels of the respective protein and conducted immunoprecipitations in analogy to

the SILAC samples to analyze the eluates for the proteins of interest. An important difference between the SILAC IP experiment and the IP for sample validation was the scale. While the SILAC IP was conducted with 80-100 mg total cell lysate, only 20 mg of the total cell lysate were employed for sample validation. The eluates of the BaF3 SILAC samples analyzed on immunoblot were fractions of the samples analysed by mass spectrometry. Due to the different scale of the immunoprecipitation, the SILAC samples were thus three-fold more concentrated than the remaining samples judged according to the intensity of Bcr-Abl on the immunoblot.

Immunoblots were developed using either near-infrared fluorescence with the Odyssey[®] imager (Licor) or enhanced chemiluminescence (ECL) depending on the signal strength. The quantified signals in the eluates of the immunoprecipitation was normalized for the Bcr-Abl level (bait) in the IP but not corrected for the total protein expression level in order to minimize sources of errors from different blots.

Validation of the pY phosphoproteomics dataset was conducted by immunoblot employing the total cell lysates of the samples used in the SILAC experiments plus the human cell lines specified in Supplementary Table S3. The human cell lines were lysed in a denaturing Urea buffer in analogy to the SILAC samples. The quantified phosphoprotein signals were normalized for the total protein expression level of the respective protein. In contrast, different Bcr-Abl expression levels were not taken into account.

In vitro kinase activity assay

Cells were lysed in TAP buffer and insoluble materials removed by centrifugation (10 min, 4°C, 20 000 xg). Total Bcr-Abl protein levels were determined by immunoblot. For immunoprecipitation, Bcr-Abl inputs levels were adjusted to 3 mg of total protein from the BaF3 p210 cell line as reference. Bcr-Abl was immunoprecipitated using 50 µL NHS-coupled anti-Abl antibody per sample. The samples were washed twice with 1 mL TAP buffer and once in kinase assay buffer (20 mM Tris-HCl pH 7.5, 10 mM MgCl₂, 1 mM DTT). Each IP sample was split into 3x 150 µL and 2x 250 µL aliquots for

kinase assay and immunoblot control, respectively. For the kinase assay, the beads with the immunoprecipitated protein were resuspended with 10 μ L kinase assay buffer, and the reaction was started by adding the assay premix. An optimal Abl peptide was used as substrate and was included in the 4x kinase assay premix (final assay concentration: 20 μ M ATP (GE healthcare, #27-2056-01), 0.33 μ M [γ - 32 P]-ATP (10 mCi/mL, 3.3 μ M, Hartmann analytic), 100 μ M Abl peptide (preferred c-Abl substrate carrying an N-terminal biotin (biotin-GGEAIYAAPFKK-amide)). The premix was added to the immunoprecipitated Bcr-Abl/Abl proteins and incubated at room temperature for 12 min. The reaction was terminated by adding 12.5 μ l of 7.5 M guanidinium-hydrochloride. A total volume of 8 μ L were spotted onto a SAM2 Biotin Capture membrane (Promega) and further treated according to the manufacturer's instructions. Incorporated γ - 32 P was quantified using a scintillation counter. The raw counts were corrected for the amount of immunoprecipitated Bcr-Abl protein as controlled by immunoblot of the IP samples and enabled determination of the relative kinase activity. To allow comparison between the different samples, the activity levels were normalized to either KCL22 or BV173 according to the level of Bcr-Abl in the IP.

Kinase activity profiling using PamChip

We probed global kinase activity in lysates of Bcr-Abl expressing BaF3 cells using the PamChipTM technology of PamGene (<https://www.pamgene.com/en/pamchip.htm>). This kinase-activity-profiling assay consists of a flow-through micro-array system with immobilized peptide sequences that can be phosphorylated by kinases in the sample. The peptide sequences cover many known signaling molecules with a set of 142 sequences for Ser/Thr phosphorylation (STK assay) and 142 sequences for Tyr phosphorylation sites (PTK assay). Phosphorylation events are quantified using FITC-labeled antibodies. The assay was performed in collaboration with the company PamGene that received the cell lysates from our laboratory.

In our experiment, we compared the kinase activity in lysates of parental BaF3 cells with that of p210- and p190-Bcr-Abl expressing BaF3 cells and

additionally added a lysate of imatinib-treated p190 BaF3. Cells were grown to an approximate density of 2.5×10^6 cells/mL. Imatinib was added 4 h prior harvesting at a concentration of 20 μ M. Cells were harvested at 500 xg and washed twice in PBS. Cell lysis was done in M-PER mammalian extraction buffer (PIERCE catalogue no. 78503) including 1x HALT protease inhibitor (PIERCE catalogue no. 87786) and 1x HALT phosphatase inhibitor (PIERCE catalogue no. 78420) and lysates were cleared by centrifugation at 16 000 xg for 15 min. Aliquots were stored and shipped at -80°C .

Interactome data analysis and hit filtering

The total protein analysis from the cell lysates (input) enabled quantification of more than 5000 proteins. Such important analysis depth allowed us covering approximately 80% of proteins quantified in the immunoprecipitate (IP) samples. This high overlap ensured robust pairwise comparison of the three labelled biological samples (H/L, M/L, H/M, according to labeling scheme in Supplementary Table S1). The overall ratio distribution for all three comparisons in the input and IP was normalized to zero and tested for significance (Significance B test in Perseus)⁷ for both replicates individually. All proteins with a significance B value <0.05 were considered as significantly, differentially quantified. Proteins that were differentially quantified in both biological repeats were represented in a scatter plot (Supplementary Figure S1). Correlation of the two IP replicates was tested and revealed a Pearson correlation coefficient greater than 0.73.

In a first filtering step, we extracted lists of proteins that are differentially quantified and enriched with Bcr-Abl as compared to the parental control in both biological replicates comprising a total of 342 proteins. All of these proteins that are significantly enriched with either p210 or p190 were subsequently normalized for their input levels by subtracting the input ratio from the IP ratio. An important advantage of the input normalization is that proteins that are carried over in the IP due to their high abundance in the input are corrected. Normalization for the input thus allowed us to distinguish true interactors from abundant background proteins or contaminants but also

lowered the impact of interactors that were already up-regulated in the input thereby reducing the risk of overestimating the extent of interaction. In contrast, no correction could be done for those proteins that were not quantified in the input. This applied to approximately 20% of the dataset.

After input normalization, we selected 147 out of the 342 proteins according to the highest ratio as compared to the parental control as well as biological knowledge. The list of proteins that were differentially quantified in the comparison of the p210 versus the p190 isoform was thus limited to these 147 proteins. This filtering option greatly facilitated further data analysis. In addition to ratio normalization with the input level of the respective proteins, we further corrected our dataset for different Bcr-Abl amounts in the IPs. In both biological replicates p210 Bcr-Abl was immunoprecipitated in slightly higher amounts than p190 Bcr-Abl (Supplementary Figure S1). For the determination of the relative Bcr-Abl levels, all peptides from common region of the two isoforms were taken into account. The correction for Bcr-Abl amounts is important, as higher amounts of bait proteins would overestimate the amount of interactor. Finally, we selected all proteins that have a log₂ ratio greater than 1 or smaller than -1 in at least one of the experiments for further analysis. Proteins with log₂ ratios between -1 and 1 in both experiments were discarded as well as those with opposite trends in the two experiments.

Phosphoproteome data analysis and hit filtering

Tyrosine phosphosites with a localization probability greater than 0.75 (Class I) were selected for the study. A large portion of the quantified phosphosites were up-regulated in the two Bcr-Abl cell lines as compared to the BaF3 parental control cell line (Supplementary Figure S5, comparing unnormalized protein and phosphosite ratios). Normalization of the parental sample was thus done for the total protein population only to account for mixing inaccuracies. Changes compared to the parental control (M/L and H/L) were depicted in a heatmap with unsupervised hierarchical clustering of the normalized log₂ ratios. In order to define a phospho motif for the common Bcr-Abl signature (clusters 2 and 3 of the heatmap), a pattern search was

performed using the MotifX software⁸ with the default parameters choosing our whole py dataset as background.

Furthermore, to allow an accurate comparison of the two Bcr-Abl isoforms, these samples were normalized not only to the total protein population but additionally the whole population of phosphosites was re-centered to zero. Initial filtering of the differential phosphosites between the p190 and p120 sample was done prior normalization of the protein abundance as this would point out signaling nodes that are enriched in the respective cell lines. We used both a statistical test (Significance B test in Perseus)⁷ as well as a static cut-off of $\log_2 \pm 1$ to group phosphorylation sites into three categories of confidence: Category 1, phosphopeptides with SignB < 0.05 in both experiments; Category 2, phosphopeptides with SignB < 0.05 in only one experiment; and Category 3, phosphopeptides not highlighted in the significance test but with an at least two-fold regulation in at least one of the experiments (marked +++, ++ and +, respectively in Supplementary Table S8). All peptides showing an opposite enrichment in the two experiments were excluded from the analysis. We then also conducted normalization to the individual protein levels to account for changes in the expression level between the two cell lines. This step allowed us to correlate phosphorylation changes to the abundance of the protein and add the phosphorylation stoichiometry as additional information. We therefore grouped phosphorylation sites into four sub-groups: group 1, phosphosites that are elevated due to a change in protein abundance; group 2, phosphosites that are elevated due to stoichiometric changes; group 3, phosphosites that are stoichiometrically different but are of lower abundance, group 4 (n.a.) is not accessible due to missing input information.

Data Analysis and MS raw data

Detailed lists of all interactors and phosphosites are provided in Supplementary Tables S4-S8 and an annotated Excel file with complete data. Network analysis has employed the DAVID bioinformatic resources for KEGG and GO term enrichment^{9,10}, STRING¹¹, PhosphositePlus¹² and Cytoscape¹³.

In addition, the mass spectrometry proteomics data have been deposited to the ProteomeXchange Consortium via the PRIDE partner repository with the dataset identifier PXD005149¹⁴.

Supplementary References

1. Burckstummer T, Bennett KL, Preradovic A, Schutze G, Hantschel O, Superti-Furga G, *et al.* An efficient tandem affinity purification procedure for interaction proteomics in mammalian cells. *Nat Methods* 2006; **3**: 1013-1019.
2. Schiff-Maker L, Burns MC, Konopka JB, Clark S, Witte ON, Rosenberg N. Monoclonal antibodies specific for v-abl- and c-abl-encoded molecules. *J Virol* 1986; **57**: 1182-1186.
3. Wisniewski JR, Zougman A, Nagaraj N, Mann M. Universal sample preparation method for proteome analysis. *Nat Methods* 2009; **6**: 359-362.
4. Kulak NA, Pichler G, Paron I, Nagaraj N, Mann M. Minimal, encapsulated proteomic-sample processing applied to copy-number estimation in eukaryotic cells. *Nat Methods* 2014; **11**: 319-324.
5. Kettenbach AN, Gerber SA. Rapid and reproducible single-stage phosphopeptide enrichment of complex peptide mixtures: application to general and phosphotyrosine-specific phosphoproteomics experiments. *Anal Chem* 2011; **83**: 7635-7644.
6. Cox J, Mann M. MaxQuant enables high peptide identification rates, individualized p.p.b.-range mass accuracies and proteome-wide protein quantification. *Nat Biotechnol* 2008; **26**: 1367-1372.
7. Tyanova S, Temu T, Sinitcyn P, Carlson A, Hein MY, Geiger T, *et al.* The Perseus computational platform for comprehensive analysis of (prote)omics data. *Nat Methods* 2016; **13**: 731-740.
8. Chou MF, Schwartz D. Biological sequence motif discovery using motif-x. *Current protocols in bioinformatics* 2011; **Chapter 13**: Unit 13 15-24.

9. Huang da W, Sherman BT, Lempicki RA. Bioinformatics enrichment tools: paths toward the comprehensive functional analysis of large gene lists. *Nucleic Acids Res* 2009; **37**: 1-13.
10. Huang da W, Sherman BT, Lempicki RA. Systematic and integrative analysis of large gene lists using DAVID bioinformatics resources. *Nat Protoc* 2009; **4**: 44-57.
11. Szklarczyk D, Franceschini A, Wyder S, Forslund K, Heller D, Huerta-Cepas J, *et al.* STRING v10: protein-protein interaction networks, integrated over the tree of life. *Nucleic Acids Res* 2015; **43**: D447-452.
12. Hornbeck PV, Zhang B, Murray B, Kornhauser JM, Latham V, Skrzypek E. PhosphoSitePlus, 2014: mutations, PTMs and recalibrations. *Nucleic Acids Res* 2015; **43**: D512-520.
13. Shannon P, Markiel A, Ozier O, Baliga NS, Wang JT, Ramage D, *et al.* Cytoscape: a software environment for integrated models of biomolecular interaction networks. *Genome Res* 2003; **13**: 2498-2504.
14. Vizcaino JA, Csordas A, del-Toro N, Dianes JA, Griss J, Lavidas I, *et al.* 2016 update of the PRIDE database and its related tools. *Nucleic Acids Res* 2016; **44**: D447-456.

Supplementary Tables

Table S1: SILAC labeling scheme for interactome (BA-IP1+2) and pY phosphoproteome (pY1+2).

	<i>light</i> <i>R, K, P</i>	<i>medium</i> <i>R6, K5, P</i>	<i>heavy</i> <i>R10, K8, P</i>
<i>BA-IP 1</i>	BaF3 parental	BaF3 p210	BaF3 p190
<i>BA-IP 2</i>	BaF3 parental	BaF3 p210	BaF3 p190
<i>pY 1</i>	BaF3 parental	BaF3 p210	BaF3 p190
<i>pY 2</i>	BaF3 parental	BaF3 p190	BaF3 p210

Table S2: Interactome and pY phosphoproteome statistics. Number of differentially quantified proteins in replicate samples based on Significance B.

	pairwise comparison	LOG2 ratio positive	LOG2 ratio negative
Ba-IP1	M/L	136	97
	H/L	144	102
	H/M	99	110
BA-IP2	M/L	229	217
	H/L	218	223
	H/M	223	223
pY1	H/M	43	57
pY2	H/M	39	45

Table S3: Human cell lines used for data validation grouped according to the Bcr-Abl isoform that is expressed in these cell lines.

All cell lines were purchased from DSMZ (German Collection of Microorganisms and Cell Cultures, Braunschweig, Germany).

Bcr-Abl	cell line	cell type	DSMZ no.
p210	K562	chronic myeloid leukemia in blast crisis	ACC-10
	KU812	chronic myeloid leukemia in myeloid	ACC-378
	KCL22	chronic myeloid leukemia in blast crisis	ACC-519
	BV173	B cell precursor leukemia	ACC-20
	CMLT1	T cell leukemia	ACC-7
p190	SupB15	B cell precursor leukemia	ACC-389
	Nalm21	B cell precursor leukemia	ACC-682
	TOM1	B cell precursor leukemia	ACC-578
none	U937	histiocytic lymphoma	ACC-5

Table S4: Common Bcr-Abl interactors. Detailed information can be found in the accompanying Excel table (Sheet 'S4_common-interactors').

Gene name	ratio1 p210/par.	ratio1 p190/par.	ratio2 p210/par.	ratio2 p190/par.
Aak1	0.26	2.48	1.41	3.26
Abi1	1.51	1.77	2.10	2.22
Ap2a1	1.06	2.54	1.61	3.25
Ap2a2	1.48	2.90	2.06	3.71
Ap2b1	1.18	2.79	1.73	3.32
Ap2m1	1.30	2.71	1.41	2.90
Ap2s1	1.18	3.13	1.52	3.38
Arhgap21	2.06	1.09	1.50	0.10
Asap1	1.10	1.35	1.21	1.41
Bclaf1	0.10	4.11	2.74	-1.01
Bcr	3.49	2.14	3.86	3.00
Bmp2k	1.18	1.88	0.99	2.35
Cbl	3.67	2.18	4.85	4.26
Cblb	2.51	2.53	4.71	4.46
Cdc37	0.74	0.20	1.23	0.67
Clint1	1.32	2.40	0.59	2.10
Cyfp1	4.31	2.54	5.41	3.38
Cyfp2	1.78	2.07	2.42	2.51
Dok1	3.88	4.74	4.92	4.65
Eps15	0.53	2.73	1.07	3.32
Eps15l1	0.91	1.86	0.67	2.08
Fsip2	5.59	5.25	6.04	5.71
Ftl1;Ftl2	1.51	1.09	0.50	0.04
Fyb	1.03	0.64	1.54	1.18
Gab2	2.11	1.99	2.62	2.40
Gak	1.14	2.83	0.71	2.43
Grap	3.84	2.88	4.81	9.65
Grb2	5.18	4.47	5.76	5.27
Homer3	1.75	0.65	1.95	0.79
Inpp1	1.40	0.35	2.69	2.05
Lrrk1	3.84	3.76	4.91	5.00
Lyn	0.75	0.30	1.55	1.22
Lzts2	1.11	0.50	2.55	1.06
Map4k1	2.87	3.64	3.03	2.57
Mkln1	0.38	0.72	1.46	1.42
Mrip1	0.23	1.83	3.30	2.39
Nck2	3.12	4.27	4.38	4.56
Nckap1l	1.25	1.58	1.87	1.89
Ndufs5	0.14	-0.41	1.61	1.07
Ptpn11	1.71	1.30	2.11	1.72
Ralbp1	1.33	2.28	1.43	2.31
Rasa1	3.36	4.64	3.28	3.95
Reps1	1.34	2.13	1.29	2.33
Rin1	4.83	4.33	3.06	3.29
Shank3	1.29	1.38	1.91	1.82
Shc1	2.89	3.28	3.56	3.77
Skap2	0.93	0.51	1.58	1.00
Sos1	1.80	1.32	3.73	3.69
Sos2	0.97	0.94	3.14	4.19
Tfg	0.20	0.46	4.70	4.30
Ubash3b	4.08	1.42	6.46	2.51
Wasf2	1.40	1.40	2.48	2.09
Ywhag	0.88	0.46	0.97	0.67
Ywhah	1.00	0.60	1.06	0.66
Znf385a	1.41	1.08	1.49	0.69
	-0.04	2.15	1.59	3.28

Table S5: Differential interactors of p210 and p190. Detailed information can be found in the accompanying Excel table (Sheets 'S5_p190-interactors' and 'S5_p210-interactors')

Bcr- Abl	Gene name	Protein names	ratio1 p190/p210	ratio2 p190/p210
p190	Aak1	AP2-associated protein kinase 1	2.656	2.334
	Abcb6	ATP-binding cassette sub-family B member 6	0.808	1.446
	Actr2	Actin-related protein 2	1.844	1.351
	Ap1b1	AP-1 complex subunit beta-1	1.795	2.051
	Ap2a1	AP-2 complex subunit alpha-1	2.116	2.304
	Ap2a2	AP-2 complex subunit alpha-2	2.138	2.101
	Ap2b1	AP-2 complex subunit beta	2.146	2.227
	Ap2m1	AP-2 complex subunit mu	1.783	1.897
	Ap2s1	AP-2 complex subunit sigma	2.315	2.340
	Arpc4	Actin-related protein 2/3 complex subunit 4	1.762	1.346
	Arrb2	Beta-arrestin-2	1.613	0.805
	Bmp2k	BMP-2-inducible protein kinase	1.045	1.984
	Card9	Caspase recruitment domain-containing protein 9	1.025	0.920
	Clint1	Clathrin interactor 1	1.582	2.158
	Clta	Clathrin light chain A	0.995	1.699
	Cltb	Clathrin light chain B	1.498	1.450
	Cltc	Clathrin heavy chain 1	1.214	1.677
	Edc3	Enhancer of mRNA-decapping protein 3	1.288	1.064
	Eps15	Epidermal growth factor receptor substrate 15	2.756	2.983
	Eps1511	Epidermal growth factor receptor substrate 15-like	1.888	1.979
	Gak	Cyclin-G-associated kinase	1.875	2.484
	Gpsm3	G-protein-signaling modulator 3	1.539	0.941
	Hcls1	Hematopoietic lineage cell-specific protein	2.154	1.524
	Itsn2	Intersectin-2	1.268	1.981
	Lyn	Tyrosine-protein kinases Lyn/Bik/Hck	0.884	1.054
	Myo5a	Unconventional myosin-Va	1.414	0.943
	Nck2	Cytoplasmic protein NCK2	1.617	0.891
	Ralbp1	RalA-binding protein 1	1.630	1.652
	Rasa1	Protein Rasa1	1.893	1.108
	Reps1	RalBP1-associated Eps domain-containing	1.311	1.799
	Rps6ka1	Ribosomal protein S6 kinase	1.147	0.742
Rsbn1l	Protein Rsbn1l	0.688	1.057	
Sds1	Serine dehydratase-like	2.699	2.128	
	Uncharacterized protein FLJ45252 homolog	2.490	2.361	
p210	Bcr	Breakpoint cluster region protein	-1.026	-0.551
	Cytip	Cytohesin-interacting protein	-0.912	-1.551
	Fam107b	Protein FAM107B	-1.818	-1.307
	Kiaa1211	Uncharacterized protein KIAA1211	-1.894	-2.409
	Krit1	Krev interaction trapped protein 1	-1.013	-0.927
	Ppp1r12a	Protein phosphatase 1 regulatory subunit 12A	-1.199	-1.700
	Ppp1r18	Protein phosphatase 1 regulatory subunit 18	-2.250	-1.782
	Shank3	SH3 and multiple ankyrin repeat domains protein	-1.318	-1.488
	Sipa1	Signal-induced proliferation-associated protein 1	-1.405	-1.696
	Spta1	Spectrin alpha chain	-0.857	-1.648
	Svil	Supervillin	-0.793	-1.071
	Tprn	Taperin	-0.750	-1.462
	Ubash3b	Ubiquitin-associated and SH3 domain-containing	-2.267	-3.213

Table S6. Phospho-tyrosine (pY) sites increased in p190. Detailed information can be found in the accompanying Excel table (Sheet 'S6_p190-pYsites).

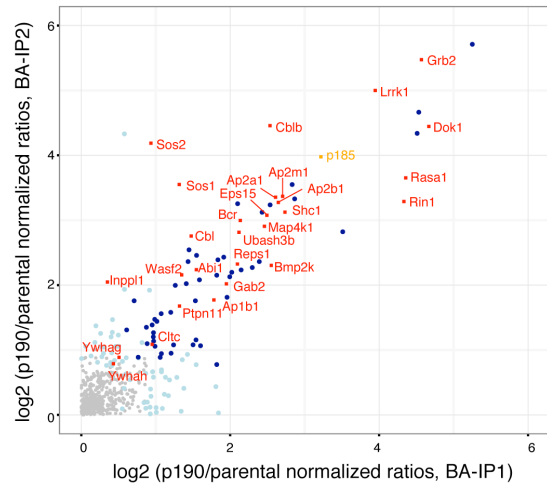
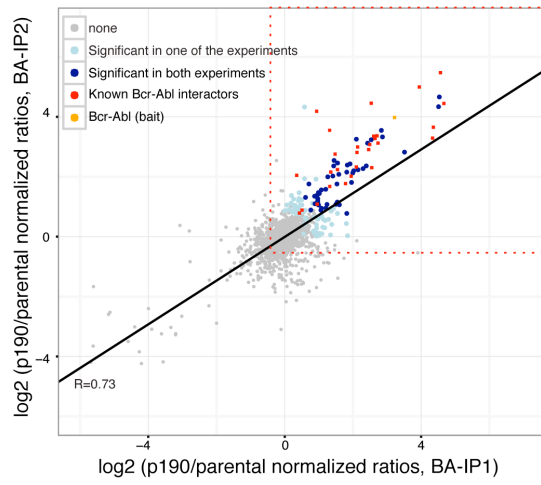
Gene names	pY position	Gene names	pY position	Gene names	pY position
Acad11	323	Guk1	53	Pag1	314
Actn1;Actn4	246;266	Hspe1	76	Peak1	528
Adss	170	Igf1r;Insr	1167;1179	Peak1	638
Agps	632	Il16	981	Peak1	879
Ahcy	193	Iqgap1	1510	Pecam1	679
Arhgap6	409	Iqgap1	654	Pecam1	702
Atxn2	260	Itn2	554	Pik3ca	246
Avil	748	Jak3	781	Ppp1cb	306
Avil	758	Lcp1	300	Ppp1r12a	496
Bub1b	397	Lst1	86	Psat1	346
Cbl	698	Lyn	306	Pstpip1	344
Cfhr2;Cfh	98; 337	Lyn	316	Ptpn11	551
Chn2	153	Lyn	397	Ptpn18	381
Cpne1	385	Lyn	473	Ptpn18	5
Dock11	57	Lyn, Blk	193	Ptpra	825
Dok1	295	Lyn, Blk	194	Ptpre	695
Dok1	314	Map1a	177	Pttg1ip	171
Dok1	397	Med30	46	Rrm1	232
Dok1	336	Mpzi1	264	Sapcd2	81
Dok1	376	Mtmr10	704	Shmt1	28
Dok1	450	Myh9	754	Skap2	237
Dyrk1a;Dyrk1b	321;273	Myh9	933	Snrnp70	146
Dyrk2;Dyrk4	380;379	Nars	550	Syncrip	276
Dzip3	1080	Nars	424	Tes	240
Eif1a	106	Nck2	50	Tgm2	582
Elp3	329	Nckipsd	161	Tjp2	1095
Eno1;Eno2	25;25	Nedd9	165	Tkt	275
Eprs	690	Nedd9	176	Tln1	436
Eps8l2	681	Nedd9	240	Tln1	70
F2r	425	Nedd9	260	Tmem154	160
Fam195b	41	Nedd9	316	Tnk2	40
Fcer1g	76	Nedd9	344	Tnk2	842
Fyb	559	Nedd9	91	Tnk2	875
Gart	417	Nfya	265	Vta1	280
Gsk3b;Gsk3a	216;279	Pag1	183	Zranb2	167

Table S7. Phospho-tyrosine (pY) sites increased in p210. Detailed information can be found in the accompanying Excel table (Sheet 'S7_p210-pYsites).

Gene names	pY position	Gene names	pY position	Gene names	pY position
Abi1	23	Emg1	61	Psm2	101
Acly	672	Exosc6	40	Psm5	220
Ahcy1	28	FAM120A	429	Psm8	184
Alms1	2903	Farsa	337	Ptbp3	98
Anxa5	92	Fes	713	Ptk2b	580
Arpp19;Ensa	59;64	Fkbp4	220	Rbck1	328
Ass1	133	Fkbp4	411	Sept7	318
Bank1	671	Fryl	2814	Shank3	930
Bank1	629	Fyn;Fgr	185;168	Siglec5	561
Brk1	63	Gab2	603	Slamf1	288
C130026l21Rik	82	Gab3	542	Stat3	704
Cacybp	200	Gab3	569	Stat5a	90
Cap1	418	Gemin8	167	Stat5a	694
Cat	231	Hspa4l	589	Stat5a	682
Cat	84	Ica1	261	Stat5a/b	668
Cd2ap	88	Ifitm3	20	Stat5b	699
Cdc23	353	Inpp1	1161	Stat5b	90
Crk	108	Ints7	935	Tbl1x	459
Csk	64	Iqgap1	172	Tgm2	219
Csrp1	71	Ist1	43	Tgm2	369
Csrp1	73	Larp4	64	Tgm2	44
Ctage5	497	Lck	192	Tgm2	617
Ctnnd1	96	Mapk1	185	Tnrc6b	1164
Dapp1	139	Mapk3	205	Tom1l2	404
Dctn3	67	Muc13	562	Tomm34	54
Ddx20	757	Nek7	289	Tuba1c	282
Ddx3x	301	Nfatc2	348	Tuba4a;Tuba1b	282
Ddx6	313	Nhp2l1	32	Tuba4a;Tuba1b;	312;312;31
Diap1;Diaph1	1069;1104	Pag1	386	Tuba4a;Tuba1b;	272;301;27
Eif2s1	147	Paics	22	Ube2e1;Ube2e3;	77;91;85
Eif2s1	150	Pdlim5	251	Uqcrc2	207
Eif3l	40	Pfcp	446	Usp4;Usp15;Usp	915;926;88
Eif3l	415	Phpt1	90	Vim	117
Eif4a1	197	Pik3ap1	570	Vim	38
Eif4g2	128	Pkp4	424	Vim	53
Eif4h	7	Prdx1	10	Wibg	45
Eif6	113	Prkcd	64		

Supplementary Figures

a p190/parental



b p210/parental

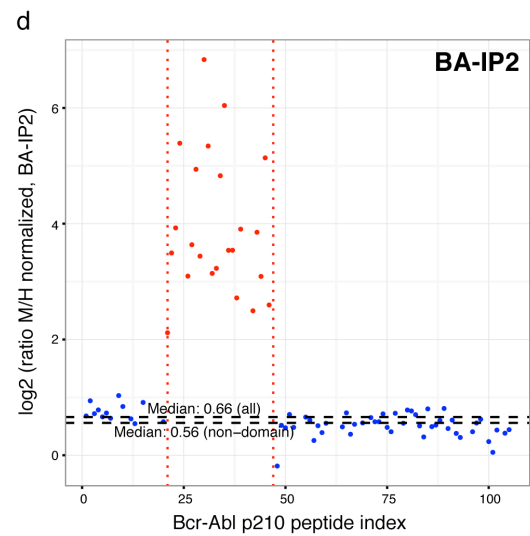
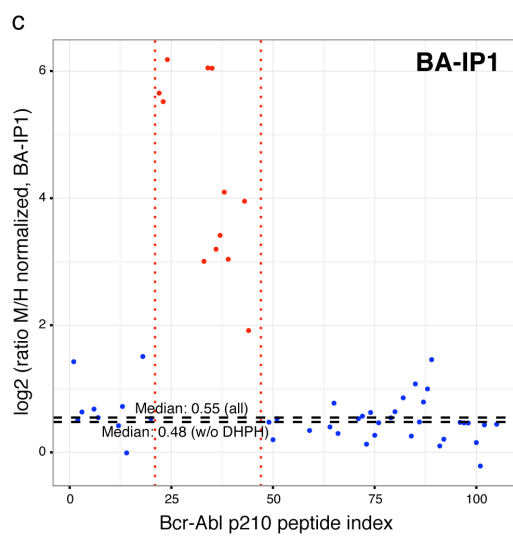
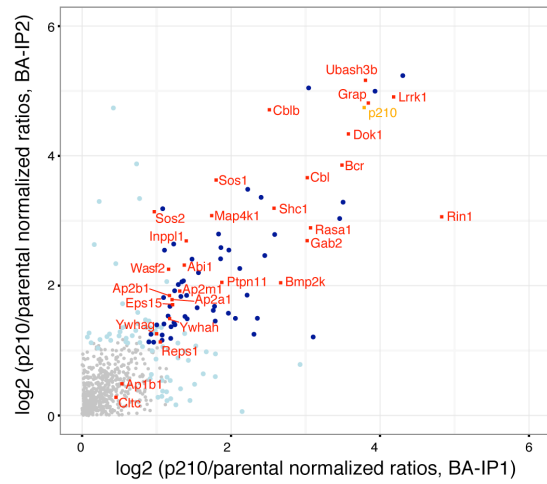
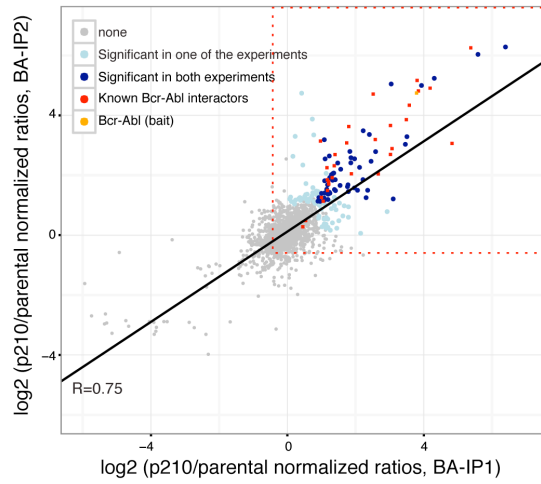


Figure S1: Mass spectrometry interactome data. (a) Scatter plot depicting the replicate pairwise comparison of the p190 sample with the parental control. Proteins that are enriched with p190 Bcr-Abl are color-coded according to their significance (blue and light blue). The already known interactors are depicted in red and additionally labeled with the gene name in the zoomed view on the right side. (b) In analogy to a, these scatter plots represent the replicate pairwise comparison of the p210 sample with the parental control. (c, d) Unique peptides of Bcr-Abl used for the quantification of the two isoforms in BA-IP1 (c) and BA-IP2 (d). Peptides that belong to the DHPH domain of p210 were excluded from the analysis.

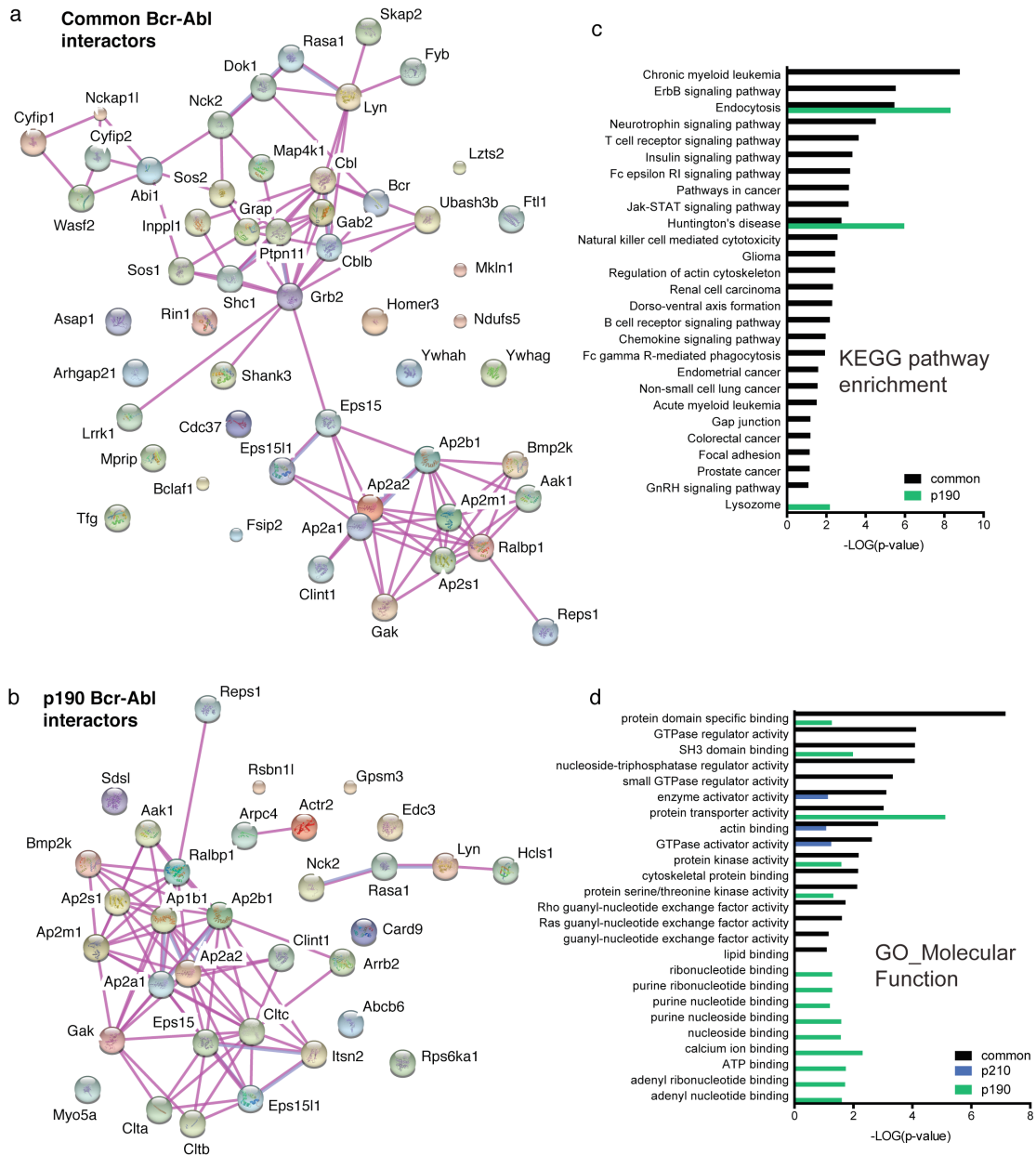


Figure S2: Bcr-Abl interactome analysis. (a) The STRING database was employed to illustrate the high experimental connectivity between the common Bcr-Abl interactors. Pink lines represent experimental evidence for interaction. (b) The proteins that preferentially and exclusively bind to p190 Bcr-Abl are represented in this network analysis using STRING, where pink lines represent experimental evidence for interaction. (c, d) Common, p210- and p190-enriched proteins were included into a KEGG pathway and gene ontology enrichment analysis using DAVID (<https://david.ncifcrf.gov/home.jsp>). The set of p210-enriched proteins did not result in a significantly enriched KEGG pathway.

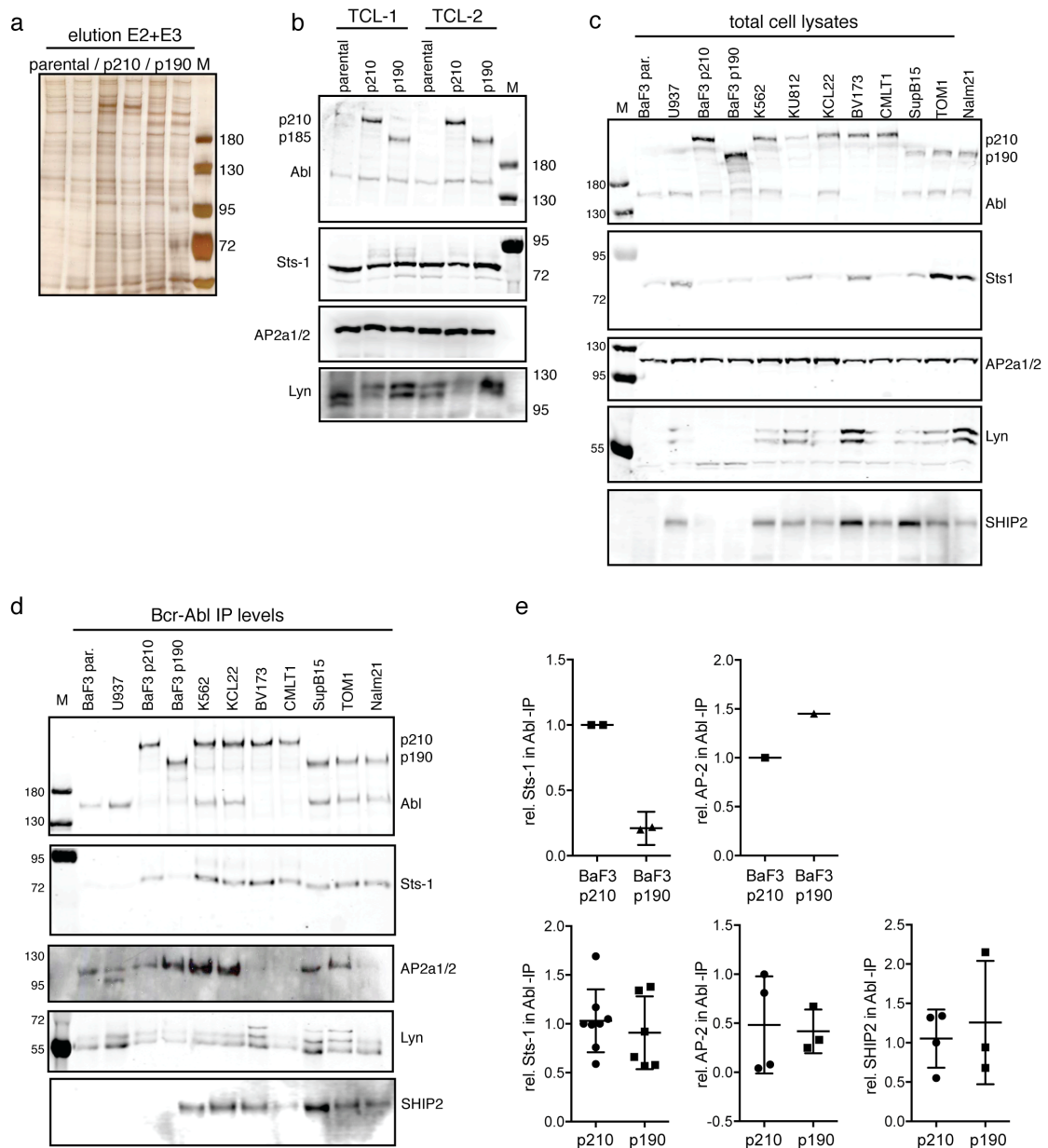


Figure S3. Interactome data validation. (a) Silver-stained SDS-PAGE of elution fractions 2 and 3 before mixing of BA-IP1. A band for each Bcr-Abl isoform can be identified and multiple additional proteins are co-purified in each sample. (b, c) Expression levels of selected proteins for interactome validation are probed in total cell lysates of the BaF3 cells (b) and the human cell lines (c). Differential expression levels are not taken into account for immunoblot quantification of the immunoprecipitates. (d) Bcr-Abl/Abl immunoprecipitation was also performed for the human cell lines and an independent set of BaF3 cells. IP eluates of these cell lines were adjusted for

Bcr-Abl amounts and the equalized samples are analyzed for the presence of Bcr-Abl/Abl, Sts-1, AP2a1/2, Lyn and SHIP-2. (e) Signals are quantified and corrected for Bcr-Abl amounts. To illustrate possible quantitative differences between the Bcr-Abl isoforms, human cell lines were grouped according to the Bcr-Abl isoform that they express.

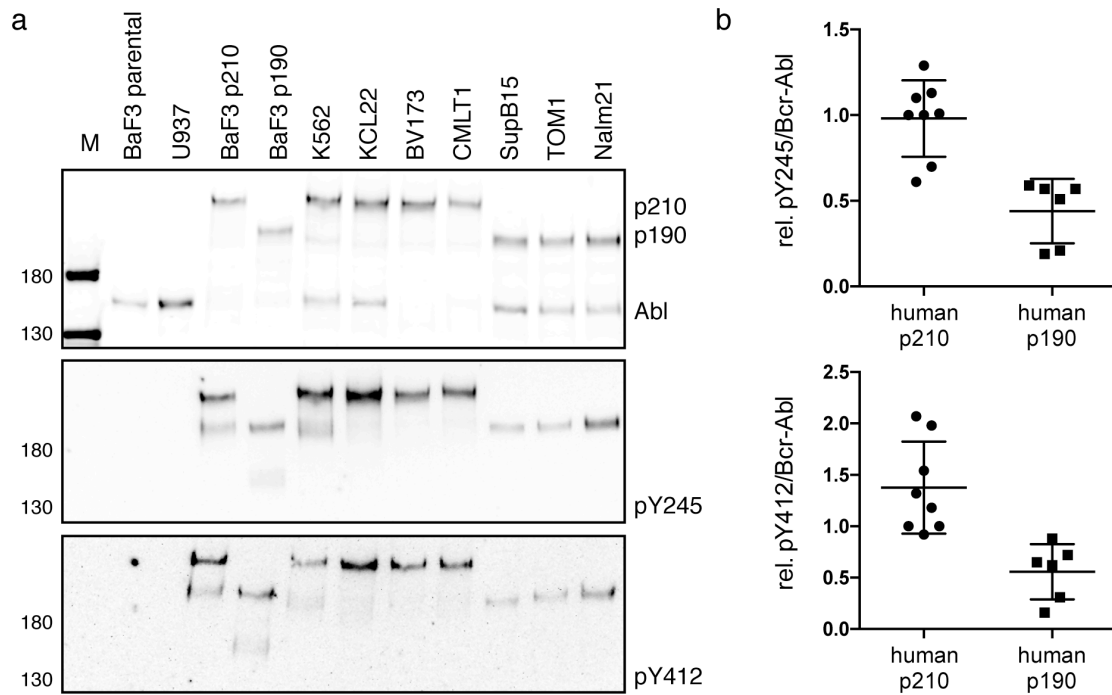


Figure S4. Phosphorylation of Bcr-Abl. (a) The equalized IP samples used for interactome data validation were also probed by immunoblot for Bcr-Abl phosphorylation on sites Y245 and Y412. While a decent signal could be obtained on Bcr-Abl itself, Abl phosphorylation is below the limit of sensitivity and cannot be observed. Quantification of the human cell lines grouped according to the Bcr-Abl isoform is shown in (b).

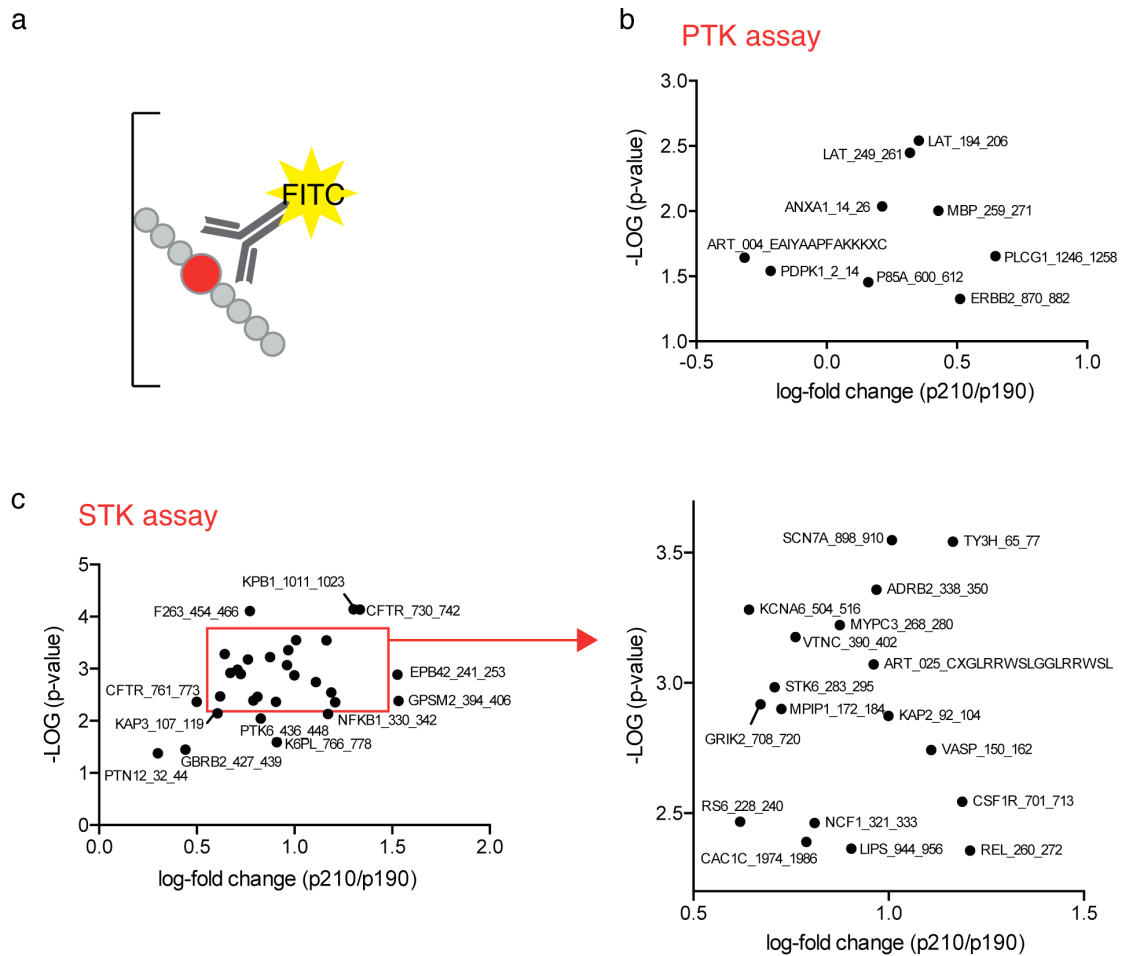


Figure S5. Kinase activity profiling using the PamChip®. (a) The principle of the assay relies on the recognition of the phosphorylated peptide by an anti-phospho-Ser/Thr or anti-phospho-Tyr antibody that carries a fluorescent label for quantification. (b) Result of the Tyrosine kinase array (PTK). The peptides that were significantly, differentially phosphorylated in the comparison of the p190- and p210-expressing BaF3 cell lysate are shown. (c) Results of the Serine/threonine kinase array (STK). The peptides that were significantly, differentially phosphorylated in the comparison of the p190- and p210-expressing BaF3 cell lysate are shown with an additional focus on the most crowded region pointed out by the red box.

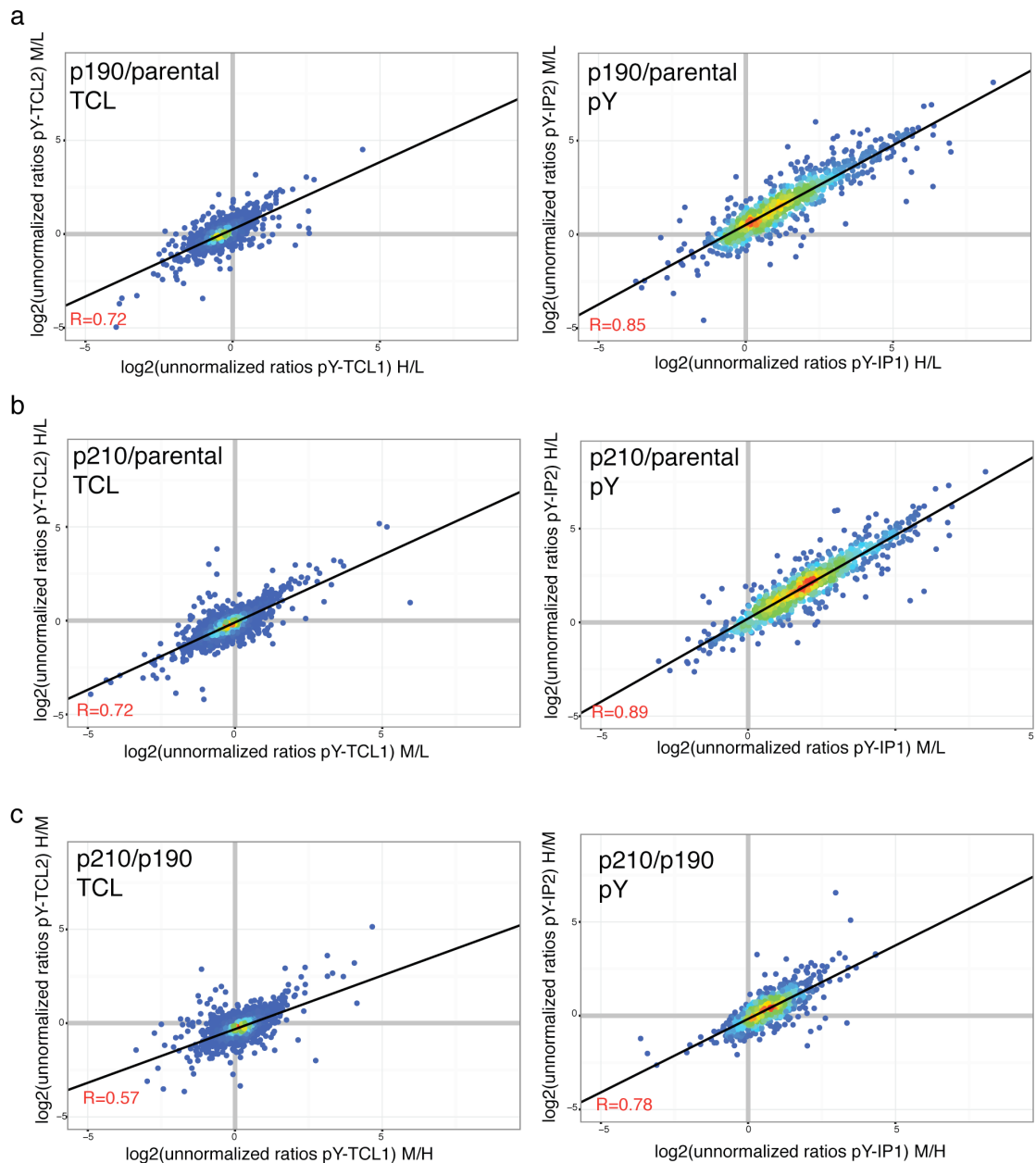


Figure S6. Tyrosine phosphoproteome MS data. (a-c) Scatter plots of unnormalized log₂ ratios in the total proteome analysis (TCL: total cell lysate, left) and after phosphotyrosine enrichment (pY, right). The graphs illustrate the large changes in phosphorylation in the presence of Bcr-Abl when compared to the parental control (a-b) without influences of the normalization procedure. In contrast the difference between the two Bcr-Abl isoforms (c) is only marginal.

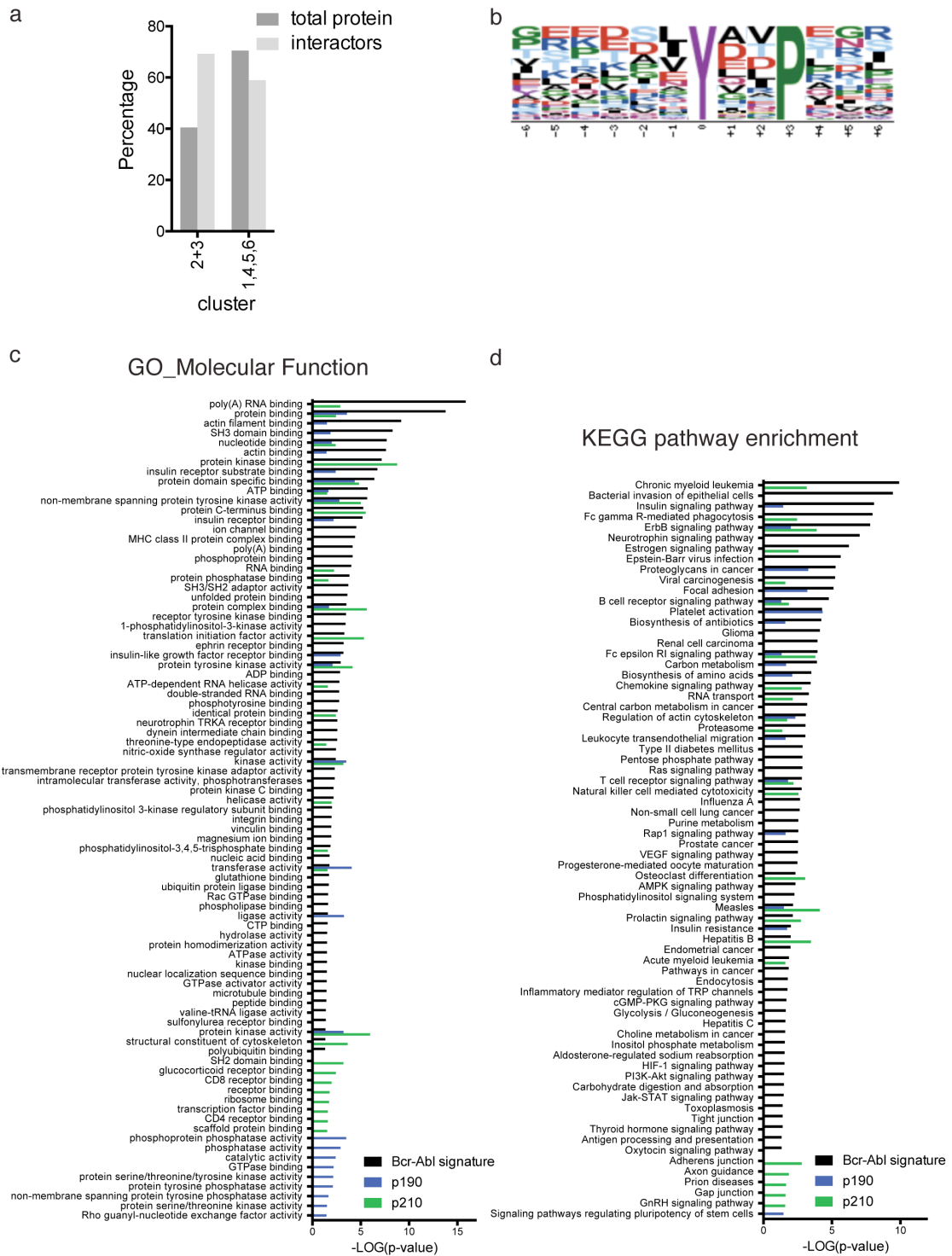


Figure S7. Analysis of the pY phosphoproteome. (a) Interactor mapping on pY data set presented in Fig. 5. The bar graph depicts the percentage of interactors found in the respective clusters versus the total number of proteins within the clusters. Interactors are overrepresented in cluster 2 and 3 that comprise the Bcr-Abl signature.

(b) Phospho motif analysis for the common Bcr-Abl signature comprised in cluster 2 and 3 versus the complete dataset. The YxxP motif was identified 67 out of 273 unique peptides representing a 4.3-fold increase.

(c,d) Functional annotation of proteins from either the Bcr-Abl signature, p190 or p210-enriched sites was computed in DAVID (<https://david.ncifcrf.gov/home.jsp>) with a focus on the gene ontology enrichment term 'Molecular function' (c) and KEGG pathway enrichment (d).

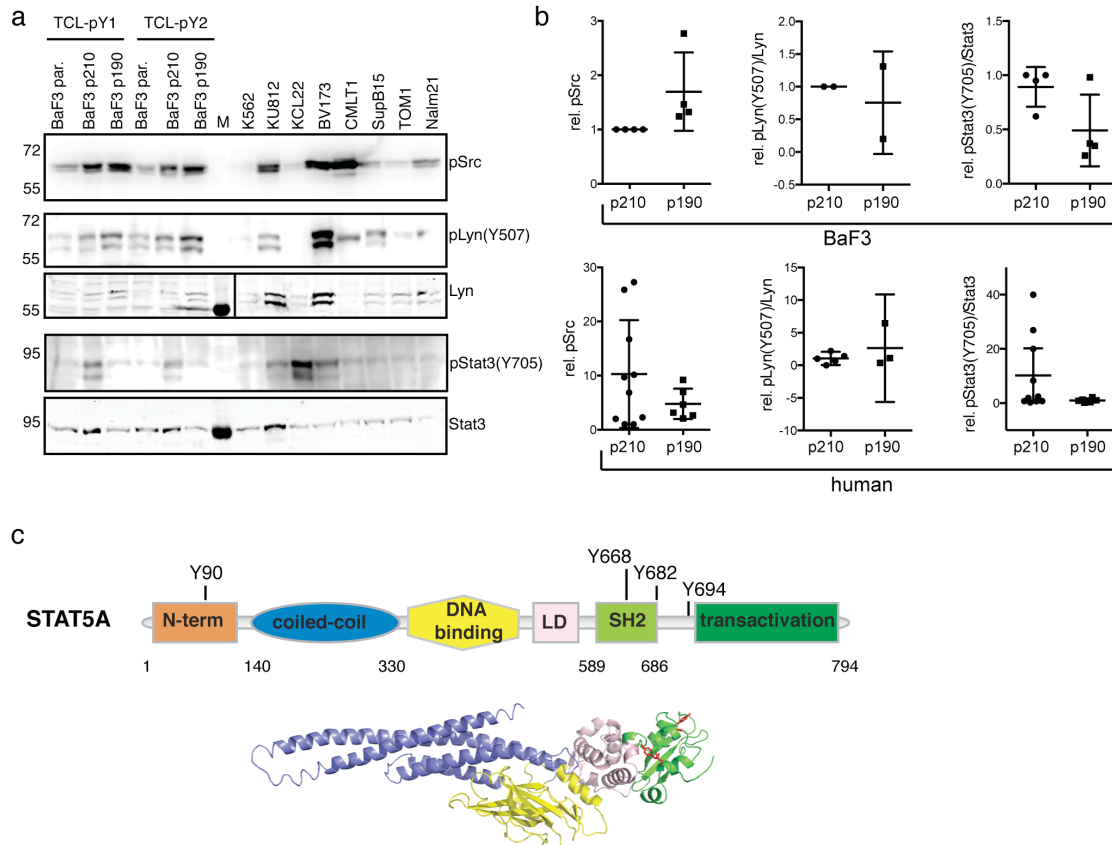


Figure S8. Validation and interpretation of the pY phosphoproteome data. (a) Immunoblot analysis of the total cell lysates of the BaF3 cell lines used for mass spectrometry as well as the human cell lines. We probed for Src activation loop phosphorylation (pSrc), the inhibitory, C-terminal phosphorylation site of Lyn (Y507) and the main phosphorylation site of Stat3 (Y705). To normalize the Lyn and Stat3 signal, total levels of the proteins were assed as well. (b) Quantification of the immunoblot signals are shown for BaF3 cells and human cell lines that were grouped according to the respective Bcr-Abl isoform. (c) Stat5a domain organization and structure (PDB ID 1y1u). The tyrosine phosphorylation sites identified by mass spectrometry are depicted on the schematic domain organization of Stat5a with an N-terminal domain, coiled-coil domain, DNA-binding domain, linker domain (LD), SH2 domain and transactivation domain. The only structure available for Stat5 comprises a core fragment without N-terminal and transactivation domain. The two phosphorylation sites found within the SH2 domain (Y668 and Y682) are highlighted with red sticks representation.